IJIREEICE

ISSN (Online) 2321-2004
ISSN (Print) 2321-5526

International Journal of Innovative Research in
Electrical, Electronics, Instrumentation and Control Engineering

Vol. 9, Issue 6, June 2021

DOI 10.17148/IJIREEICE.2021.9633

Classification of Bone Lesion Instance using Bone Scintigraphy under Semi-Supervised Learning

Nancy Chitra Thilaga.N[1], Thangavelammal.R[2], Vijaya.K[3] , Thamizharasi.P[4], Muthumuniyammal.M[5]

Assistant Professor, Electronics and Communication Engineering, Grace College of Engineering, Thoothukudi, India[1]

Student, Electronics and Communication Engineering, Grace College of Engineering, Thoothukudi, India[2,3,4,5]

Abstract: The lack of labelled data poses a main challenge in applying deep learning to medical imaging. Despite of the availability of large amounts of clinical data, it is difficult to acquire labelled image data, in particular for bone Scintigraphy (i.e. 2D bone imaging). This paper presents a neural network model that can classify bone cancer metastases in the chest area in a semi supervised manner. This deep learning model, classifies each instance independently, utilizes global information through an additional connection from the core network thereby achieving higher accuracy.

Keywords: Bone Scintigraphy, Neural Network, Semi-supervised learning, Clinical Imaging

I. INTRODUCTION

Currently there are about 1.7 million people diagnosed with cancer every year. Cancer has been detected in multiple organs and it can rarely be cured after spreading to the bones. Thus the detection of bone cancer plays a critical role in the diagnosis and treatment of the condition. Bone scintigraphy is a nuclear medicine procedure that uses radioactivity to perform bone cancer imaging. Because the spread of cancer often manifests in bones, clinicians usually request bone scintigraphy results before proceeding with the treatment. The bone scintigraphy results play a vital role as supporting information for primary decision-making during screening and for identifying the positions of any abnormal regions, called lesions . However, abnormalities found in bone scans include not only cancer but also other bone abnormalities that can be considered benign. A malignant lesion is characterized as a cluster of dangerous tumor cells that can lead to bone cancer metastases .

II. BACKGROUND

To judge whether a lesion is malignant, the nuclear medicine expert must consider characteristics such as pixel intensity (which reflects the level of radioactive uptake),lesion location, number of lesions, etc. In cases where lesion categorization is difficult due to ambiguous characteristics, the time a physician spends during diagnosis to interpret the results may increase by up to an hour or more per patient. Consequently, using machine learning to support this task could help improve efficiency, resulting in better diagnosis. The glitches involved in applying machine learning to medical imaging applications lie in the need for manual labeling. Labeling bone scintigraphy data requires nuclear medicine physicians, making the labeling task expensive and time-consuming. Thus, it is highly likely that only a small portion of the available data will be labeled. Furthermore, when labeling physicians are uncertain about the type of lesion, they may label more than one class per lesion (multilabel data), making the data labeling complex. The current instance segmentation methods are designed for supervised learning and require large amounts of labeled data for training; they cannot use unlabeled data, and ends up in poor efficiency when the labeled dataset is small.

III. PROPOSED METHOD

The proposed model is a neural network to perform lesion instance segmentation. Although lesions can occur anywhere throughout the body, they are often found in the chest area which is often the hardest to diagnose as it consists of small bones, due to the complexity and overlap of the ribs. Therefore, the focus is mainly on finding lesions in the chest area. Fig1 and Fig 2 shows the block diagram and the overview of the proposed system. We start by locating the chest area using the single shot multibox detector (SSD) [in both anterior and posterior whole-body views in the bone scintigram. The SSD is a one-stage detection model that can bse trained and makes inferences at high speed.

IJIREEICE

ISSN (Online) 2321-2004
ISSN (Print) 2321-5526

International Journal of Innovative Research in
Electrical, Electronics, Instrumentation and Control Engineering

Vol. 9, Issue 6, June 2021

DOI 10.17148/IJIREEICE.2021.9633

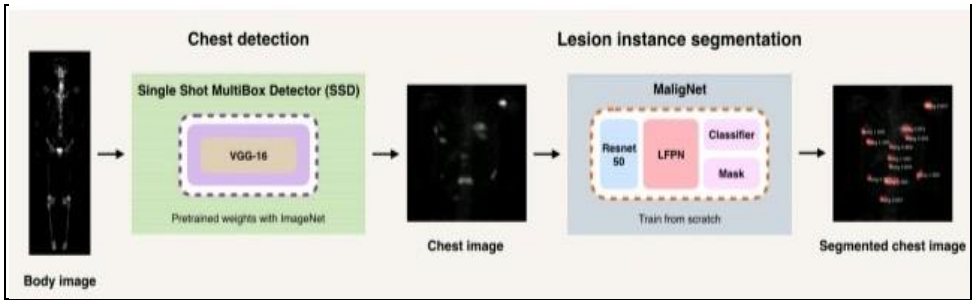

Fig.1 Block Diagram of the proposed system

Conventionally, object detection for natural images is performed by detecting each object independently—regardless of the other objects in the same image. However, physicians usually consider both other lesions and additional cues beyond the lesion itself when determining the lesion types. For example, if a lesion is isolated, without other nearby lesions, it is more difficult to assert that the isolated lesion is malignant. However, when multiple lesions occur in the same region, they are possibly malignant. The Convolutional Neural Network model has been used where the ladder feature pyramid network has been added to the top-down pathway to allow semi-supervised training. An additional layer which extracts global features from the core network to the classifier head has also been added.

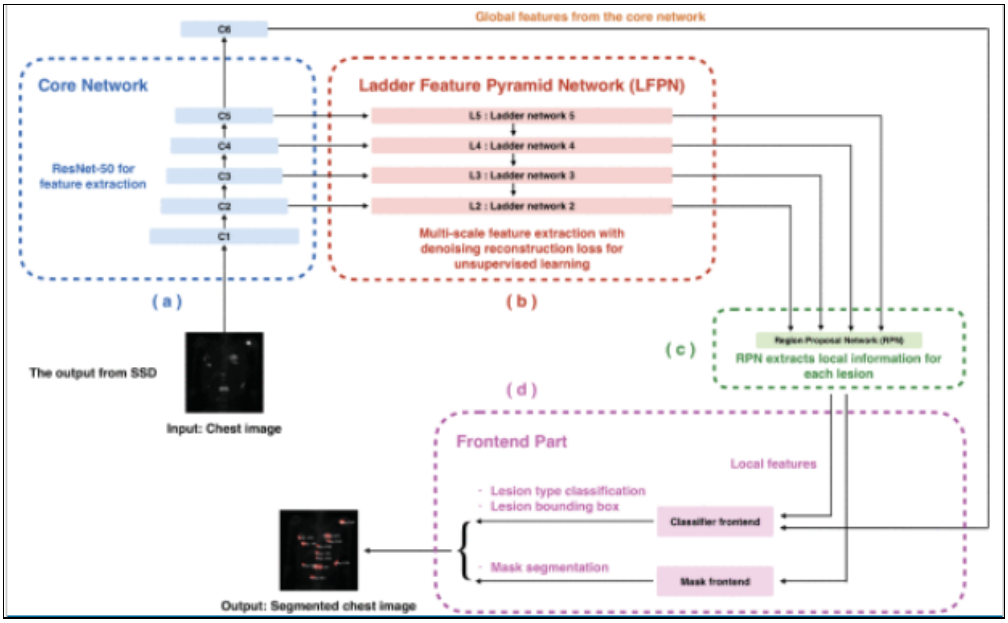

Fig.2 Overview of the system

A.Feature Pyramid Network

The Feature pyramid network(FPN) detects objects at different scales, which is the case for lesions in a chest image. An FPN consists of two main parts: bottom-up and top-down pathways. The bottom-up path way is the feed forward neural network, which can be any object classifier. The top-down pathway, which is connected to the bottom up pathway through lateral connections, is designed to build semantic feature maps at multiple scales by double
up scaling to enhance the feature maps from the bottom-up pathway.

B.Region proposal net

A region proposal network (RPN) is a type of fully convolutional network that is used in Faster R-CNN. This model is part of a region-based family that includes R-CNN, Fast R-CNN and Mask R-CNN. Region-based object detectors first identify potential regions for objects and then classify each region into object classes.

C.*Ladder Network*

A ladder network is a semi supervised learning method, that can utilize labeled and unlabeled data simultaneously. It is similar in concept to a de noising auto encoder (DAE). A DAE is an auto encoder that receives a

IJIREEICE

ISSN (Online) 2321-2004
ISSN (Print) 2321-5526

International Journal of Innovative Research in
Electrical, Electronics, Instrumentation and Control Engineering

Vol. 9, Issue 6, June 2021

DOI 10.17148/IJIREEICE.2021.9633

corrupted data point as input and is trained to reconstruct the uncorrupted data point. A ladder network takes this a step further by introducing noise at every layer, not just the input. Fig 3 illustrates a simple ladder network.

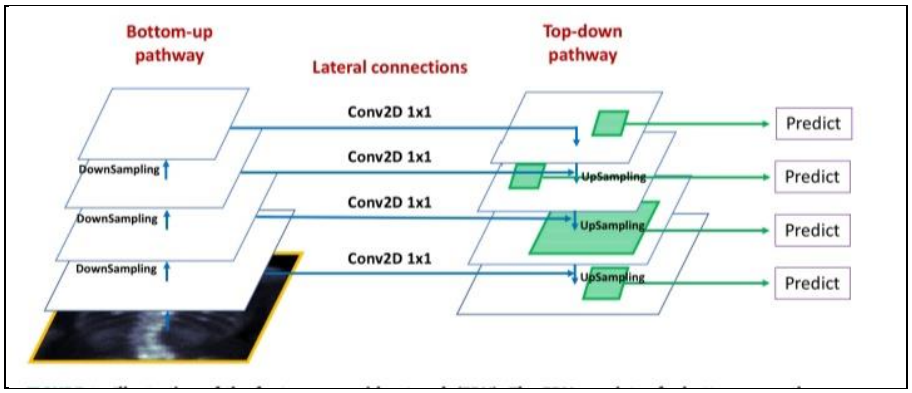

Fig 3 Illustration of Feature Pyramid Network

The dataset was separated into training, validation, and testing data as listed in Table 1. The physician focused on four main lesion types: malignant (or cancerous), infection/inflammation, degenerative change(bone deterioration), and post trauma (broken regions caused by accidents).

Table 1 Number of labelled and unlabelled training data for Lesion Instance Segmentation

Data type	Amount of data	Training Data	Validation data	Testing data
Labelled data	1,088	741	231	116
Unlabelled data	18,560	14,786	3,774	0
Total data	19,648	15,527	4,005	116

The numbers of each type of lesion are shown in Table 2.

Table 2 Total number of lesions per type

Lesion Types	Number of Lesions
Malignant	3,500
Inflection/ Inflammation	290
Degenerative change	805
Post-traumatic	415
Total Lesions	5,010

IV. RESULT

A.Results of Chest Detection

Anterior (front-side) and posterior (back-side) images are available for each patient. Because detecting the chest area in the whole image from bone scintigraphy is a simple task, the model provides accurate results: its min, mean, and max Jaccard indexes are 0.804, 0.933, and 0.987, respectively.

IJIREEICE

ISSN (Online) 2321-2004
ISSN (Print) 2321-5526

International Journal of Innovative Research in
Electrical, Electronics, Instrumentation and Control Engineering

Vol. 9, Issue 6, June 2021

DOI 10.17148/IJIREEICE.2021.9633

Fig 4 Examples of Chest detection model

The first bone scintigram in Fig 4 (the leftmost side) is an anterior view (front view), and the second bone scintigram is a posterior view (back view) of a pediatric patient. The third skeleton is an anterior view, and the last skeleton (the rightmost side) is a posterior view of an adult patient. The ground-truth boxes are indicated in green, while the outputs of the SSD model are indicated in red. The Jaccard indices from left to right are 0.895, 0.943, 0.987, and 0.914.

B.Results of the Lesion Instance Segmentation task

The chest images from bone scintigraphy (the output results from chest detection), were used as the input data in this task. Data cleaning and augmentation were applied before performing the experiments. We evaluated our model on the lesion instance segmentation task for the four lesion types and compared the results with the baseline model (Mask R-CNN). Fig 5 shows the confusion matrix of the lesion classification task. The rows represent the true labels (ground truth), and the columns represent the predicted labels

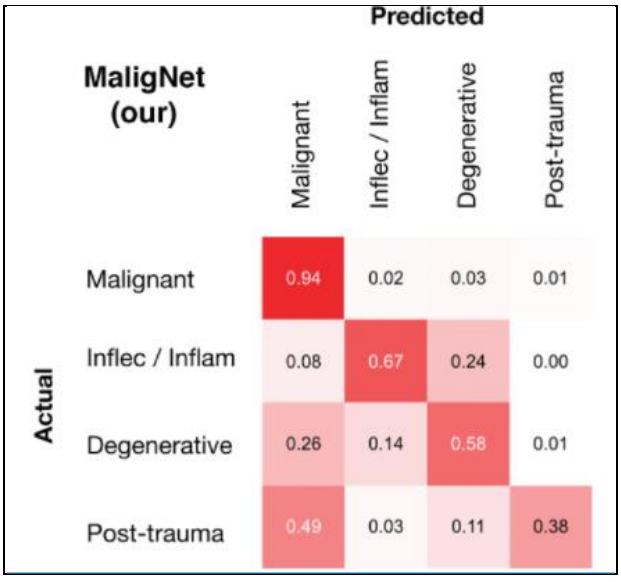

Fig 5 Confusion matrix of Lesion Classification task

C.The Impact Of Data

To study the effectiveness of unsupervised learning in the semi-supervised approach in leveraging unlabeled data, models were trained with varying amounts of labeled and unlabeled data and measured their performances.

IJIREEICE

ISSN (Online) 2321-2004
ISSN (Print) 2321-5526

International Journal of Innovative Research in
Electrical, Electronics, Instrumentation and Control Engineering

Vol. 9, Issue 6, June 2021

DOI 10.17148/IJIREEICE.2021.9633

D.Effect of The Amount Of Labeled Data

The amount of labeled training data was varied while keeping the amount of unlabeled data fixed and measuring the F1-score as shown in Fig 6. Using unsupervised data, the model without global features improves every time the amount of training data is increased, thus it outperforms the Mask R-CNN baseline model by an average of 1.51%. Adding the global features improves the performance even further, reaching a relative F1-score average improvement of 2.40%. At the same F1-score level, the proposed method reduces the amount of labeled data required by an average of 20.11%.

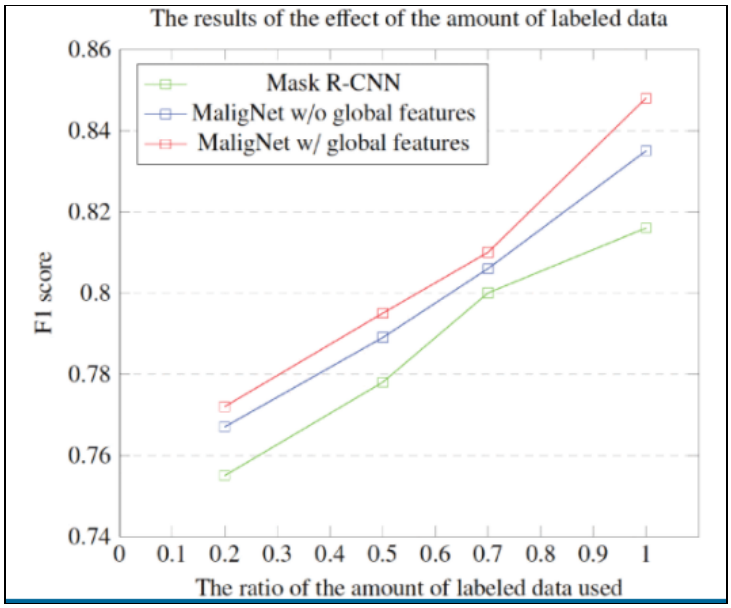

Fig 6 Effect of amount of labeled data in lesion instance segmentation measured by F1-score

E.Effect Of The Amount Of Unlabeled Data

The effect of varying the amount of unlabeled data was studied. The performance increases as we include more unlabeled training data. However, at higher amounts, the gain from adding more data decreases. This is expected because the unlabeled data are used to learn better representations. When the model has captured sufficient variation from the unsupervised data, adding more unsupervised data will have little to no effect.

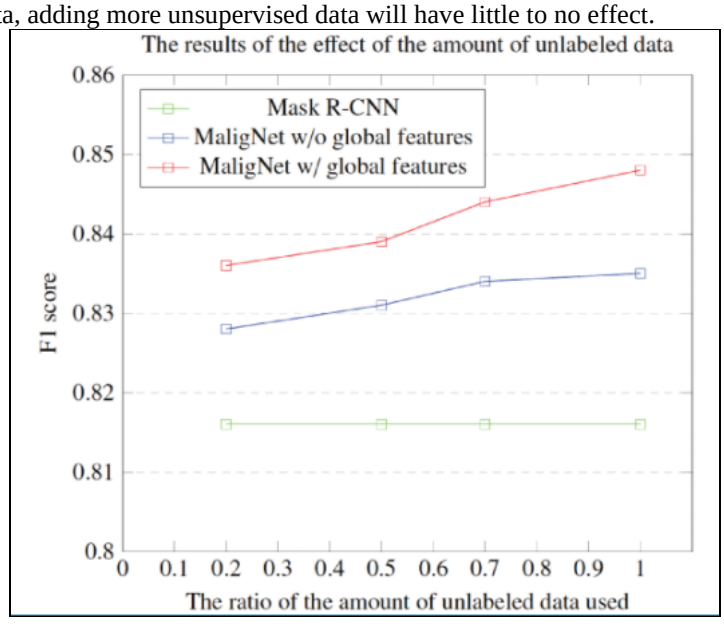

Fig 7 Effect of amount of unlabeled data in lesion instance segmentation measured by F1-score.

IJIREEICE

ISSN (Online) 2321-2004
ISSN (Print) 2321-5526

International Journal of Innovative Research in
Electrical, Electronics, Instrumentation and Control Engineering

Vol. 9, Issue 6, June 2021

DOI 10.17148/IJIREEICE.2021.9633

The Fig 8 and Table 3 shows the ROC analysis for the proposed model and that the accuracy of the classification task.

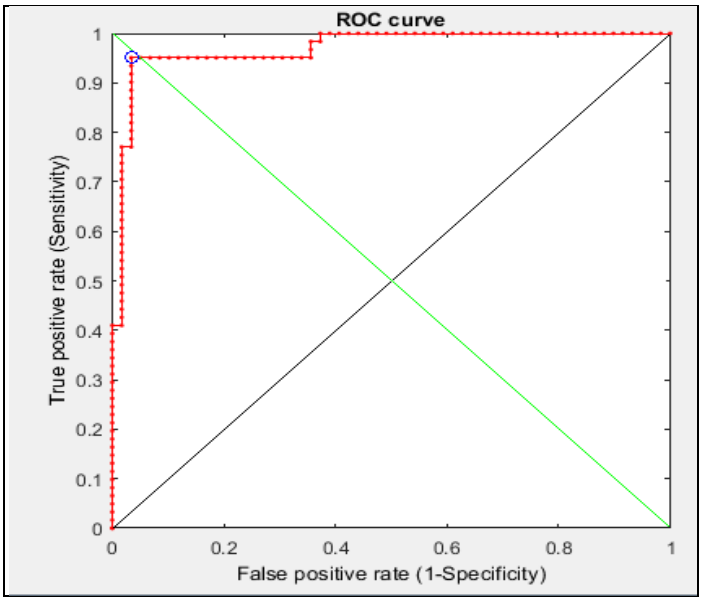

Fig 8 ROC Image

Table 3 ROC Curve Analysis

AUC	S.E.	95%	C.I.	COMMENT
0.96999	0.1591	0.93880	1.00000	EXCELLENT TEST

V. CONCLUSION

The proposed model is a single network that is simple, effective, flexible, and lightweight. Normally, semi-supervised models must be trained using multiple steps. This model provides an end-to-end solution that can be trained in one step with both labeled and unlabeled data simultaneously, which reduces the training time. The input data are bone scintigraphy images, which have similar patterns, characteristics, and compositions, unlike general images. For this reason, we can take advantage of the specificity of the data, enabling the model to learn good representations of bone scan images from unlabeled data. Furthermore, applying global features helps to classify the lesion types based on the overall composition of the image, more closely mimicking the diagnostic approach of physicians

In further analyses, we plan to visualize the model to determine what the model sees and the reasons why it makes its categorizations. We also plan to apply our model to other domains e.g., MRI and CT. We believe that this method provides an alternative approach for handling unlabeled data and will be useful in applications for other works.

REFERENCES

[1]. F. Ambellan, A. Tack, M. Ehlke, and S. Zachow, ‘‘Automated segmentation of knee bone and cartilage combining statistical shape knowledge and convolutional neural networks: Data from the Osteoarthritis Initiative,’’ Med. Image Anal., vol. 52, pp. 109–118, Feb. 2019.

[2]. R. Azmi, N. Norozi, R. Anbiaee, L. Salehi, and A. Amirzadi, ‘‘IMPST: A new interactive self-training approach to segmentation suspicious lesions in breast MRI,’’ J. Med. Signals Sens., vol. 1, no. 2, p. 138, 2011.

[3]. L. Belcher, ‘‘Convolutional neural networks for classification of prostate cancer metastases using bone scan images,’’ Dept. Astron. Theor. Phys., Lund, Sweden, Tech. Rep., 2017.

[4]. T. Bradshaw, T. Perk, S. Chen, H.-J. Im, S. Cho, S. Perlman, and R. Jeraj, ‘‘Deep learning for classification of benign and malignant bone lesions in [F-18] NAF PET/CT images,’’ J. Nucl. Med., vol. 59, no. 1, p. 327, 2018.

[5]. M. Bustamante, V. Gupta, D. Forsberg, C.-J. Carlhäll, J. Engvall, and T. Ebbers, ‘‘Automated multi-atlas segmentation of cardiac 4D flow MRI,’’ Med. Image Anal., vol. 49, pp. 128–140, Oct. 2018.

[6]. V. Cheplygina, M. De Bruijne, and J. P. Pluim, ‘‘Not-so-supervised: A survey of semi-supervised, multi-instance, and transfer learning in medical image analysis,’’ Med. Image Anal., vol. 54, pp. 280–296, May 2019. [7] C. B. Confavreux, J.-B. Pialat, A. Bellière, M. Brevet, C. Decroisette, A. Tescaru, J. Wegrzyn, C. Barrey, F. Mornex, P.-J. Souquet, and N. Girard, ‘‘Bone metastases from lung cancer: A paradigm for multidisciplinary onco-rheumatology management,’’ Joint Bone Spine, vol. 86, no. 2, pp. 185–194, Mar. 2019.

[7]. M. Courbariaux, I. Hubara, D. Soudry, R. El-Yaniv, and Y. Bengio, ‘‘Binarized neural networks: Training deep neural networks with sweights and activations constrained to +1 or −1,’’ 2016, arXiv:1602.02830. [Online]. Available: https://arxiv.org/abs/1602.02830

[8]. J. Dang, ‘‘Classification in bone scintigraphy images using convolutional neural networks,’’ M.S. thesis, Lund Univ., Math. (Fac. Eng.), Lund, Sweden, 2016.

IJIREEICE

ISSN (Online) 2321-2004
ISSN (Print) 2321-5526

International Journal of Innovative Research in
Electrical, Electronics, Instrumentation and Control Engineering

Vol. 9, Issue 6, June 2021

DOI 10.17148/IJIREEICE.2021.9633

[9]. B. D. D. Vos, J. M. Wolterink, P. A. D. Jong, M. A. Viergever, and I. Išgum, ''2D image classification for 3D anatomy localization: Employing deep convolutional neural networks,'' Proc. SPIE, vol. 9784, Mar. 2016, Art. no. 97841Y

[10]. J. Deng, W. Dong, R. Socher, L.-J. Li, K. Li, and L. Fei-Fei, ''ImageNet: A large-scale hierarchical image database,'' in Proc. IEEE Conf. Comput. Vis. Pattern Recognit., Jun. 2009, pp. 248–255

[11]. M. Everingham, L. Van Gool, C. K. I. Williams, J. Winn, and A. Zisserman, ''The Pascal visual object classes (VOC) challenge,'' Int. J. Comput. Vis., vol. 88, no. 2, pp. 303–338, Jun. 2010